

# A study of cathode catalysis for the aluminium/hydrogen peroxide semi-fuel cell

Russell R. Bessette<sup>a,b,c,\*</sup>, James M. Cichon<sup>a,b,1</sup>, Dwayne W. Dischert<sup>b,c</sup>, Eric G. Dow<sup>b</sup>

<sup>a</sup> Department of Chemistry and Biochemistry, University of Massachusetts Dartmouth, North Dartmouth, MA 02747, USA

<sup>b</sup> Electric Propulsion Branch-Code 8231, Naval Undersea Warfare Center (NUWC), Newport Division, Newport, RI 02841, USA

<sup>c</sup> Systems Integration and Research, One Corporate Place, Middletown, RI 02840, USA

## Abstract

The characterization and use of a Pd and Ir catalyst combination on a C substrate in an Al/H<sub>2</sub>O<sub>2</sub> semi-fuel cell is described. The Pd–Ir combination outperforms Pd alone or Ir alone on the same substrate. Scanning electron microscopy (SEM) and energy dispersive spectrophotometry (EDS) were used to establish the location of Pd, Ir and O in clusters on the cathode substrate surface. X-ray photoelectron spectroscopy (XPS) binding energy measurements indicate that Pd is in the metallic state and the Ir is in the +3 state. A configuration consisting of an Ir(III) oxide (Ir<sub>2</sub>O<sub>3</sub>) core and a Pd shell is proposed. The electrochemical, corrosion, direct and decomposition reactions which take place during cell discharge were evaluated. Improved initial and long term performance, at low current densities, of the Al/H<sub>2</sub>O<sub>2</sub> semi-fuel cell incorporating a Pd–Ir on C cathode relative to a similarly catalyzed Ni substrate and a baseline silver foil catalyst is demonstrated. © 1999 Elsevier Science S.A. All rights reserved.

**Keywords:** Aluminium anode reserve cells; Semi-fuel cells; Catalysis

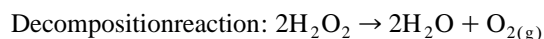
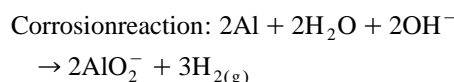
## 1. Introduction

Aluminium anodes used in aqueous batteries with, for example, Ag(II) oxide or air cathodes have been investigated extensively [1]. The use of a H<sub>2</sub>O<sub>2</sub> catholyte in combination with an Al anode has been the subject of several studies carried out by the electric propulsion group at NUWC [2,3]. When Al is combined with H<sub>2</sub>O<sub>2</sub> in a caustic electrolyte, the overall cell reaction is:



Operating cell voltages in the 1.2–1.7 V range, depending on current density, have been routinely obtained. The Al/H<sub>2</sub>O<sub>2</sub> electrochemical couple compares favorably with the Al–AgO couple and other high-energy-density primary battery systems. An energy density of 360 W h dm<sup>-3</sup> is likely to be achievable for the Al/H<sub>2</sub>O<sub>2</sub> solution phase catholyte system whereas an energy density of 290 W h dm<sup>-3</sup> is projected for a similarly configured Al–AgO system [2].

An ion diffusion membrane is not used in the semi-fuel cells studied, in order to reduce complexity, weight and cost and increase reliability and cell voltage. This approach, however, results in the catholyte being in direct contact with both the anode and the electrocatalytic cathode substrate. A direct, non-electrochemical, reaction will thus occur. Unless the rate of this direct reaction is low compared to the electrochemical anodic and cathodic reactions, the direct reaction will significantly reduce the overall efficiency of the cell. Additional reductions in efficiency can occur due to the corrosion reaction of Al with hydroxide ions and the decomposition reaction of H<sub>2</sub>O<sub>2</sub>.



Improved catalysis for the reduction of H<sub>2</sub>O<sub>2</sub> should result in reductions of the direct and the decomposition reactions thus improving significantly the electrochemical efficiency of the cell.

Several catalysts have been investigated for use in fuel cells [4]. Many of these catalysts (including Pd and Ir independently) have been incorporated in C based pastes [5]. Collman and Kim [6] have reported that iridium porphyrin complexes are very active catalysts. Cox and Ja-

\* Corresponding author. Department of Chemistry and Biochemistry, University of Massachusetts Dartmouth, North Dartmouth, MA 02747, USA

<sup>1</sup> Present Address: Duracell Worldwide Technology Center, 37 A Street, Needham, MA 02494, USA.

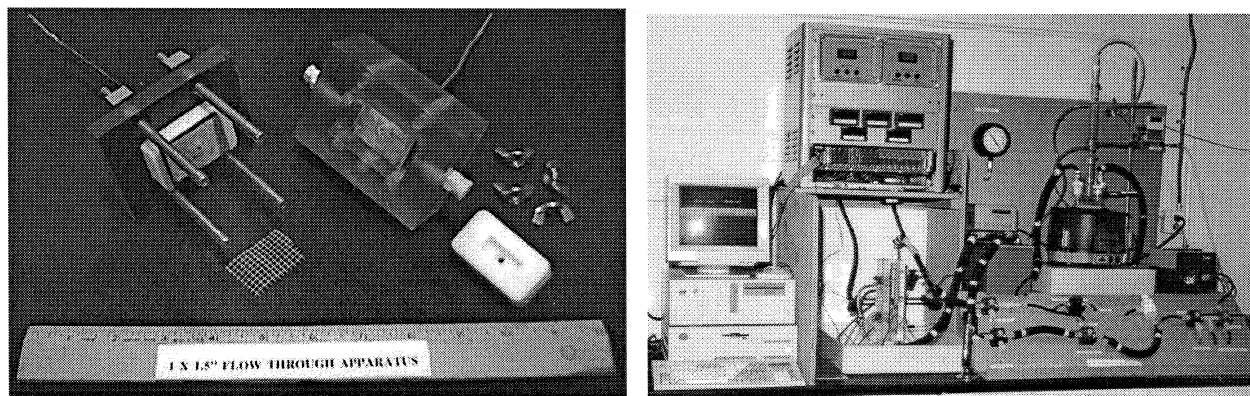


Fig. 1. Flow-through test cell apparatus.

worski [7] have used a Pd–Ir combination on a glassy C microelectrode for the quantitative determination of  $\text{H}_2\text{O}_2$ . A combination of Pd and Ir has been shown in the NUWC Electric Propulsion Laboratories to improve the electrochemical efficiency for the reduction of  $\text{H}_2\text{O}_2$  and to improve cell voltage relative to the use of a metallic silver cathode [8].

The studies described in this paper were directed at verification of the improved electrocatalytic behaviour of a Pd–Ir combination, at stabilizing the Pd–Ir deposit on an appropriate substrate, at determination of electrochemical, Al corrosion,  $\text{H}_2\text{O}_2$  decomposition and direct reaction efficiencies and at characterization of the catalytic surface.

## 2. Experimental

All chemicals used in this investigation were of reagent grade quality and were used as obtained from the supplier (Aldrich Chemicals or Fisher Scientific) without further purification. All solutions were prepared using glass-distilled water.

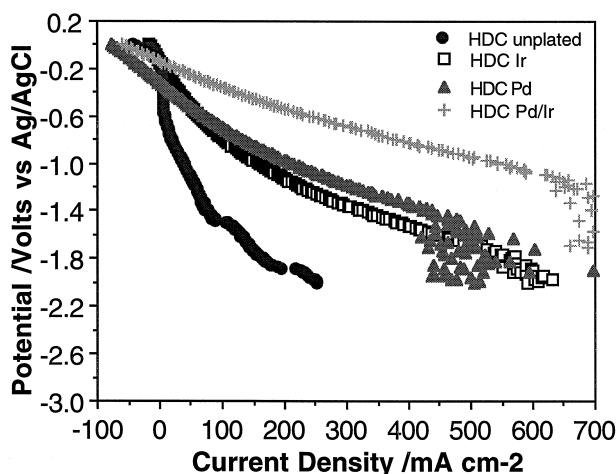


Fig. 2. Polarization curves for various catalysts used for the reduction of  $\text{H}_2\text{O}_2$ .

The simultaneous deposition of Pd and Ir on the substrate was carried out by cyclic voltammetry from  $-150$  to  $-350$  mV vs. AgCl at a rate of  $10 \text{ mV s}^{-1}$  using a EG&G Model 273A potentiostat/galvanostat and data acquisition system. The degree of loading was controlled by carrying out the deposition for exactly 20 cycles. The solution used for the deposition was heated to  $70^\circ\text{C}$  and contained  $1.0 \text{ mM PdCl}_2$ ,  $2.0 \text{ mM Na}_2\text{IrCl}_6$ ,  $0.2 \text{ M KCl}$ , and  $0.1 \text{ M HCl}$ . A three-electrode cell, consisting of the substrate (high density C or reticulated Ni) working electrode, a Ag/AgCl reference electrode and a Pt auxiliary electrode was used.

The high density C (99.95% purity,  $1.0 \text{ mm}$  thick, Goodfellow Cambridge) and reticulated Ni (Eltech;  $100 \text{ pores in.}^{-1}$ ) substrates were soaked in  $6 \text{ M HCl}$  for  $30 \text{ min}$  and rinsed with distilled water prior to use.

All polarization curves were recorded using an EG&G Instruments, Model 273A potentiostat/galvanostat and associated data acquisition system. A three-electrode cell

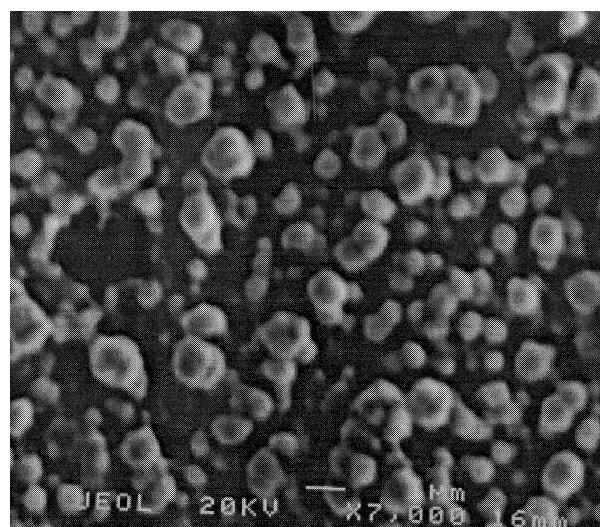


Fig. 3. A Pd–Ir combination on high density carbon at  $7000\times$  magnification.

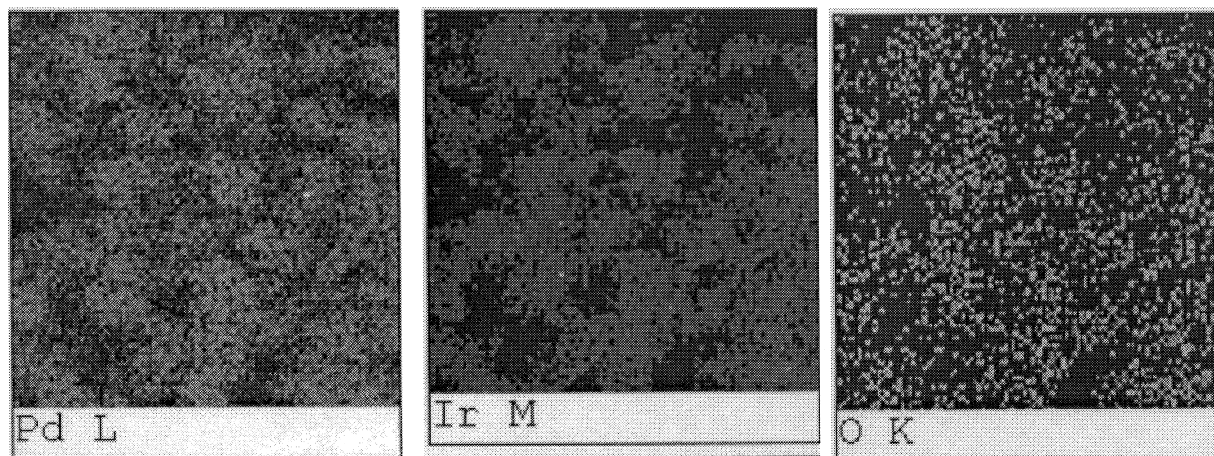


Fig. 4. EDS mapping for Pd–Ir combination on high density carbon.

consisting of the catalyzed substrate as the working electrode, a Ag/AgCl reference electrode and a spectroscopic grade carbon rod counter electrode was employed.

Full-cell performance was carried out using either a 25 × 38 mm (1" × 1.5") cell made of polycarbonate and Teflon or a 38 × 200 mm (1.5" × 8") cell made of plexi-glass (Fig. 1). The Teflon insert shown with the 25 × 38 mm cell permitted an electrode area of 1.0 cm<sup>2</sup> (5 × 20 mm<sup>2</sup>) to be used in the flow-through cell as well as a 6.25 cm<sup>2</sup> (25 × 25 mm<sup>2</sup>) electrode. A Vexar spacer maintained the cell gap at 0.7 mm in both cells. The anode and cathode were mounted on individual current collector bus bars. The two electrodes were mounted vertically and were separated by the Vexar screen spacer. The catholyte and the electrolyte were pumped into the bottom of the cell, flowed between the anode and the cathode surfaces and exited at the top of the cell. The cells were incorporated into a closed-loop flowing electrolyte apparatus consisting, in series, of a heated electrolyte reservoir, a peristaltic pump, a heat exchanging coil in a constant temperature bath to maintain temperature, the flow-through cell and a return to the reservoir. Cell current was regulated by means of a multistep load resistance substitution box and a

dynamload. Cell current, voltage, inlet and outlet temperatures, and evolved gas flow rate were simultaneously monitored and recorded by the computer data logging system. The software used for the data acquisition was Lab Tech Notebook.

The Al anode was an Alupower alloy designated EB50V. The electrolyte contained 3.0 M NaOH, 0.5 M H<sub>2</sub>O<sub>2</sub> and 40 g l<sup>-1</sup> of sea salt. Its temperature was maintained at 55°C and the flow rate was 100 cm<sup>3</sup> min<sup>-1</sup>.

Evolved gas was collected with a gas tight syringe from a T connection and rubber septum at the exit to the cell. Gas samples were taken several times during a particular run. The gas samples were analyzed for H<sub>2(g)</sub> and O<sub>2(g)</sub> with a Hewlett Packard capillary gas chromatograph Model 5890 Series II Plus equipped with an HP PLOT molecular sieve 5A column (30 m long; 0.32 mm diameter; 0.25 μm film thickness) and a thermal conductivity detector.

The scanning electron microscopy (SEM) was carried out using a JEOL USA Model 6300 instrument. The SEM working distance was 15 mm giving a resolution of 5.0 nm. A Princeton Gamma Tech energy dispersive spectrom-

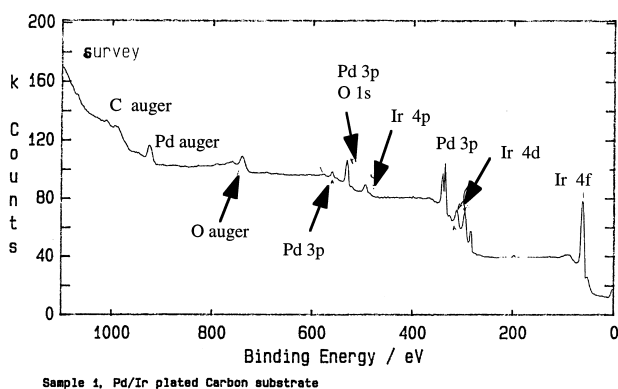


Fig. 5. XPS spectrum for a Pd–Ir combination on a carbon substrate.

Table 1  
Al/H<sub>2</sub>O<sub>2</sub> reactions

Electrochemical reaction	
$2\text{Al} + 3\text{HO}_2^- \rightarrow 2\text{AlO}_2^- + \text{OH}^- + \text{H}_2\text{O}$	(1)
Corrosion reaction	
$2\text{Al} + 2\text{H}_2\text{O} + 2\text{OH}^- \rightarrow 2\text{AlO}_2^- + 3\text{H}_{2(g)}$	(2)
Direct reaction	
$2\text{Al} + 3\text{H}_2\text{O}_2 + 2\text{OH}^- \rightarrow 2\text{AlO}_2^- + 4\text{H}_2\text{O}$	(3)
Decomposition reaction	
$2\text{H}_2\text{O}_2 \rightarrow 2\text{H}_2\text{O} + \text{O}_{2(g)}$	(4)

eter (EDS) was used for surface characterization. The detector was a digital sealed light element Si(Li) spectrometer with a beryllium window. A Sun Sparc workstation with integrated microanalyzer for Imaging and X-ray (IMIX) software was employed.

### 3. Results and discussion

A high density planar C substrate was found to support the most uniform electrocatalytic surface [9]. A comparison of the catalytic performance of Ir alone, Pd alone and a Pd–Ir combination for the reduction of  $H_2O_2$  in a sodium hydroxide-sea salt electrolyte at  $55^\circ C$  is presented in Fig. 2. The superior performance of the combination of Pd–Ir over the entire current density range is clearly evident.

A scanning electron micrograph (SEM) of the Pd–Ir combination on the C substrate at  $7000\times$  magnification is shown in Fig. 3. The clusters observed are reasonably spherical and are uniformly distributed over the substrate surface. An EDS spectrum has confirmed the presence of Pd and Ir on the surface. Oxygen was also observed but no chlorine was found. Careful analysis of EDS mapping shows the Pd, Ir and O to be at the same locations on the surface (Fig. 4).

Supporting evidence for the nature of the catalytic surface is given by the X-ray photoelectron spectroscopy (XPS) spectrum of Fig. 5. This spectrum also shows the presence of Pd, Ir and O but no Cl. Binding energy measurements indicate that Pd is in the metallic state while the Ir is in the +3 state. Toshima [10], in studying

Table 2

Reaction efficiencies for the Al/ $H_2O_2$  semi-fuel cell

Reaction	% Efficiency (Al based)	% Efficiency ( $H_2O_2$ based)
Electrochemical	$54\% \pm 4.5$	$38\% \pm 2.5$
Corrosion	$25\% \pm 1.4$	–
Direct	$23\% \pm 1.9$	$38\% \pm 0.8$
Decomposition	–	$25\% \pm 2.2$

bimetallic nanoparticles, has proposed their formation in a core shell configuration. He located the metal of the bimetallic pair with the more positive standard reduction potential in the core and the other metal in the shell. Based on Toshima's work, our EDS and our XPS data, the Pd–Ir catalyst appears to be present in two phases; one of iridium oxide ( $Ir_2O_3$ ) in the core and the other of Pd metal in the shell. Transmission electron microscopy (TEM), which can detect even smaller crystallites on the surface than XPS and which can yield complementary information, will be utilized to further characterize the catalyst.

A series of tests were carried out using the  $30\times 200$  mm flowing test apparatus to quantify the efficiencies of the four reactions which take place during the cell discharge. The corrosion, direct and decomposition reactions provide no useful electrical energy. Only the electrochemical reaction produces electrical energy (Table 1).

The Al electrochemical efficiency is determined by mass difference and integration of the current over the time of the experiment. The  $H_2O_2$  electrochemical efficiency is determined by Ce(IV) titration of the  $H_2O_2$

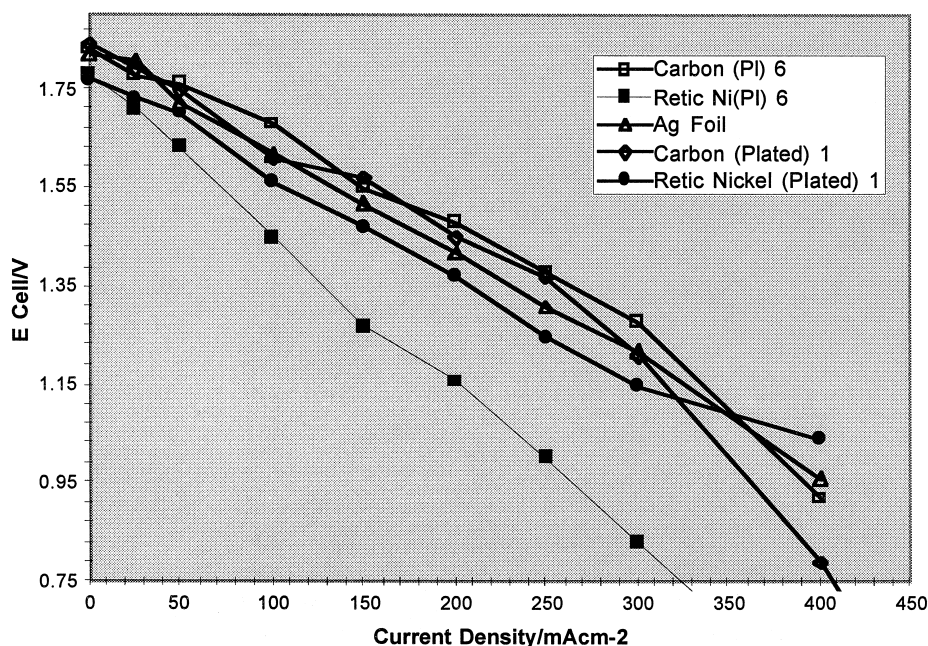


Fig. 6. Semi-fuel cell voltages at current densities up to  $400\text{ mA cm}^{-2}$  after discharges at  $100\text{ mA cm}^{-2}$  for 3.75 h and employing various catalyzed substrates.

(using 1,1-phenanthroline iron complex as the visual indicator) at the start and at the end of the experiment and by integration of the current over the time of the experiment. The Al corrosion efficiency is based on the  $H_{2(g)}$  analysis and the  $H_2O_2$  decomposition efficiency is based on the  $O_{2(g)}$  analysis. The percent direct reaction is obtained by difference.

For clarity, the definitions of the electrochemical and decomposition efficiencies are based upon the moles of  $H_2O_2$  consumed by the electrochemical and decomposition reactions, respectively, relative to the total number of moles of  $H_2O_2$  consumed. The efficiency for the corrosion reaction is defined as the mass of Al consumed by the corrosion reaction relative to the total mass of Al consumed. The electrochemical efficiency can also be determined by the mass of Al consumed in the electrochemical reaction (integration of current over time of the experiment) divided by the total mass of Al consumed. The direct reaction efficiency based on Al is obtained by subtracting the sum of the percent corrosion and percent Al electrochemical efficiencies from 100% [ $100\% - (\% \text{ corrosion} + \% \text{ Al-electrochemical})$ ]. The direct reaction efficiency can also be based on  $H_2O_2$  and is obtained, in this case, by subtracting the sum of the percent decomposition and percent  $H_2O_2$  electrochemical efficiencies from 100% [ $100\% - (\% \text{ decomposition} + \% H_2O_2 \text{ electrochemical})$ ]. These efficiencies are summarized in Table 2. The data are based on triplicate determinations.

Determination of the corrosion and decomposition reaction efficiencies has been hampered by the difficulty of obtaining dry samples of  $H_{2(g)}$  and  $O_{2(g)}$  from the electrolyte stream. Variation in electrochemical efficiency is due to the need to further optimize the electrolyte flow rate. These results indicate that an increase of 25 to 35% in the electrochemical efficiency should be achievable.

Multiple Al/ $H_2O_2$  semi-fuel cell discharges at  $100 \text{ mA cm}^{-2}$  for 45 min followed by the acquisition of cell voltages at various current densities show continued catalytic activity and stable electrochemical performance for the Pd–Ir catalyzed C substrate. Semi-fuel cell voltages at various current densities for Pd–Ir catalyzed high density planar C and reticulated Ni, obtained initially (C and Ni plate 1) and after discharge at  $100 \text{ mA cm}^{-2}$  for 3.75 h; (C and Ni plate 6), are shown in Fig. 6. The cell performance using a silver foil baseline catalyst is included for comparison.

The voltage of the cell containing the Pd–Ir catalyzed C, after 3.75 h of  $H_2O_2$  discharge, is higher than the silver foil baseline by 70 mV in the  $100\text{--}300 \text{ mA cm}^{-2}$  range and is essentially identical to its initial performance. The voltage of the cell containing Pd–Ir catalyzed reticulated Ni is lower than the baseline silver foil over the entire current range, both initially and after 3.75 h of discharge. The poorer performance of the cell incorporating catalyzed reticulated Ni after discharge relative to its initial performance is clearly evident.

Cell voltages measured at  $250 \text{ mA cm}^{-2}$  for the Al/ $H_2O_2$  semi-fuel cell containing Pd–Ir catalyzed high density C after successive discharges at  $100 \text{ mA cm}^{-2}$  for 45 min were as much as 380 mV higher than when a similarly catalyzed reticulated Ni cathode was employed. Improved long term performance was also demonstrated by the cell containing catalyzed C. The cell voltage decreased to 1.00 V after 12 45-min discharges at  $100 \text{ mA cm}^{-2}$ , whereas, the 1.00 V level was obtained after only six 45-min  $100 \text{ mA cm}^{-2}$  discharges with the cell containing catalyzed reticulated Ni.

#### 4. Conclusions

A combination of Pd and Ir on high density C shows greater catalytic activity than that obtained for either metal alone.

Scanning electron microscopy and energy dispersive spectrophotometry data indicate that Pd, Ir and O are located in spherical clusters on the surface. XPS binding energy measurements indicate the catalyst combination contains Pd in the metallic state and Ir in the +3 state. A configuration consisting of an Ir(III) oxide,  $Ir_2O_3$ , core and a Pd shell is proposed. Transmission electron microscopy will be utilized to further characterize the catalyst.

The electrochemical, corrosion, direct and decomposition reactions which take place during cell discharge were evaluated. The efficiencies based on Al and on  $H_2O_2$  are presented and indicate an increase of 25 to 35% in the electrochemical efficiency should be achievable.

Improved initial and long term performance at low current densities of an Al/ $H_2O_2$  semi-fuel cell incorporating a Pd–Ir on C cathode relative to a similarly catalyzed Ni substrate and a baseline silver foil catalyst is demonstrated.

#### Acknowledgements

The authors wish to thank the Office of Naval Research (ONR-333) for sponsorship of this project. Valuable assistance provided by colleagues at the Naval Undersea Warfare Center (NUWC) Propulsion Branch is also gratefully acknowledged.

#### References

- [1] D. Linden, Handbook of Batteries, McGraw-Hill, New York, 1984.
- [2] E.G. Dow, R.R. Bessette, G.L. Seebalch, C. Marsh-Orndorff, H. Meunier, J. VanZee, M.G. Medeiros, J. Power Sources 65 (1997) 207.
- [3] R.R. Bessette, J.M. Cichon, D.W. Dischert, Proceedings of the 38th Power Sources Conference, Cherry Hill, NJ, June, 1998.

- [4] M.G. Poirier, C. Perreault, L. Couture, C. Sapundzhiev, Proceedings of the First International Symposium on New Materials for Fuel Cell Systems, Montreal, Quebec, Canada, 1995, p. 258.
- [5] T. Okamoto, I. Baba, H. Kato, Japan Patent JP6-36784, July, 1992.
- [6] J.P. Collman, K. Kim, J. Am. Chem. Soc. 108 (24) (1986) 7847.
- [7] J.A. Cox, R.K. Jaworski, J. Anal. Chem. 61 (1989) 2176.
- [8] R.R. Bessette, J. Cichon, C. Deschenes, M. Medeiros, E. Dow, D. Dischert, NUWC unpublished results, 1998.
- [9] J. Cichon, R.R. Bessette, D. Dischert, Proc. 194th Electrochem. Soc. Meeting, Boston, MA, Nov. 2, 1998.
- [10] N. Toshima, 216th Am. Chem. Soc. National Meeting, Materials Chemistry Secretariat, 1998, Paper 19.